STUDY ON SIMULATION METHOD OF GROUNDWATER FLOW IN VARYING FLOW FIELDS

Hisashi IMAI [1)]
[1)] HAZAMA ANDO CORPORATION

ABSTRACT

The resent human activities required more effective technologies related to numerical simulation of groundwater flow. For such requirements, the groundwater simulation methods were studied to adapt to several current issues, such as the expansion of range of applied hydraulic conductivity, long term evaluation of hydrogeological features related to disposal of high level radioactive waste from nuclear power generations and so on. In this study, the following four items were studied to increase the availability of groundwater simulation to the resent requirements. 1) Methodology of boundary condition setting. 2) Measurements of unsaturated seepage parameters for rocks. 3) Estimation method of ground settlements using the results of groundwater flow simulation. 4) Simulation method to adapt the evolution of hydrogeological environments during the long time of the order of million yeas. These studies enable us to estimate groundwater behaviors and the characteristics of hydrogeological environment to match recent hydrogeological concerns.

KEYWORDS: groundwater flow, numerical simulation, boundary condition, unsaturated seepage parameters, settlement, long term evolution of hydrogeological environment

1. INTRODUCTION

The resent human activities required more effective technologies related to numerical simulation of groundwater flow. For such requirements, the groundwater simulation methods were studied to adapt to several current issues, such as the expansion of range of applied hydraulic conductivity, long term evaluation of hydrogeological features related to disposal of high level radioactive waste from nuclear power generations and so on.

1) Methodology of boundary condition setting.
2) Measurements of unsaturated seepage parameters for rocks.
3) Estimation method of ground settlements using the results of groundwater flow simulation.
4) Simulation method of long term regional groundwater flow considering the changes of hydrogeological environments.

2. METHODOLOGY OF BOUNDARY CONDITION SETTING

3.1 Background

The boundary condition setting is one of the most important issues to conduct appropriate numerical simulation of groundwater flow, because the boundary condition setting can control the direction of groundwater flow and also the amount of groundwater flow. In most of cases, the boundary conditions are determined and set before executing the simulations. But in some cases, the boundary condition can't be determined before calculation. The seepage free boundary condition is an example that can't be determined the actual boundary before calculation. Further more, there exist more complex boundary condition cases. Then three types of the complex boundary condition cases were studied and proposed the logics of determining the boundary conditions.

3.2 Complex boundary condition cases

Concerning the environmental influence evaluation related to the geological disposal of high level radioactive waste, the following three complex boundary condition cases were encountered. The images of the three cases were illustrated in Fig.1. To solve the complex boundary condition problems, procedures to determine the appropriate boundary condition was studied and developed

Case1: In case of elements are deleted from the FEM model during the progress of the excavation.
Case2: In case of evaluating the evolution of unsaturated zone around tunnel induced by the evaporation on the tunnel wall.
Case3 : In case of the slope surface that have potential to be set both flux fixed boundary

condition(recharge boundary) and head fixed boundary(seepage face boundary).

3.3 Example of the newly developed procedure

The applied result of Case1 is presented in section 5, that of Case2 is presented in the paper Imai et al (2013). Here shows an example developed for Case3 type complex boundary condition setting.

The simple slope model for the example problem was shown in Fig.2. The model was composed of two part have different hydraulic conductivity k1(=1x10^{-6}m/s) and k2(=1x10^{-7}m/s). The boundary condition on the bottom and on the left and on the right side is no-flow condition. The slope surface has the complex boundary condition. Recharge rate 100mm/y was applied on the surface.

The calculated results with newly developed procedure at steady state were shown in Fig.3 and Table1. Fig.3(a) shows the distribution of total head[m] and velocity. Fig.(b) shows the total head and recharge rate on the surface nodes. Table1 shows the node coordinate(x, z), total head, pressure head saturation, flux and recharge rate (calculated based on the node fluxes) on each surface node. The plus values for node flux and recharge imply inflow from out of model, and the minus value implies outflow from model. The colored cells on node flux column show the nodes applied the new concept boundary condition presented in Fig.1Case3 as "new". The new concept boundary condition enables us to get continual and natural flux distribution on a slope surface.

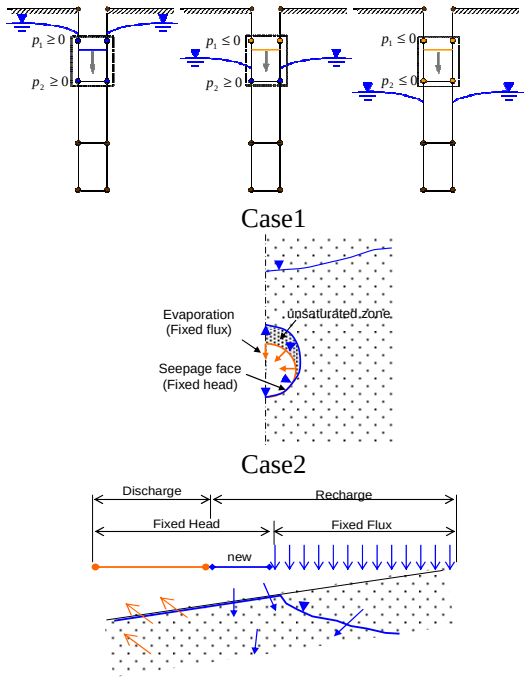

(new : new concept boundary condition)

Fig.1 Three complex boundary condition cases

Without the new concept boundary condition, the flux distribution on the surface should be discontinuous and unnatural. This example calculation presents the efficiency of the new concept boundary condition and the developed algorithms to set Case3 type new concept boundary condition.

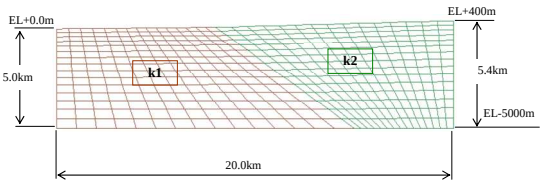

Fig.2 Configuration of the simple slope model

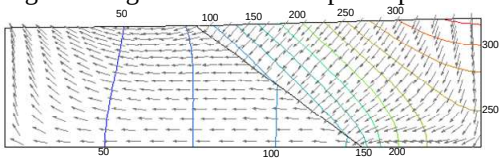

(a) Distribution of total head[m] and velocity distribution

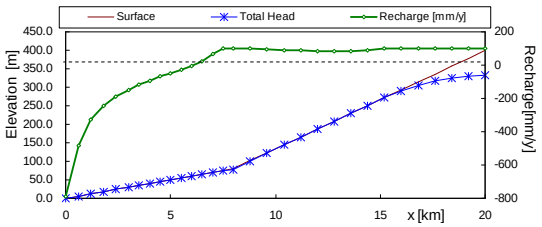

(b)Total head and recharge rate on the slope surface

Fig.3 simulated results for slope model

Table.1 The surface nodes coordinate, total head, pressure head, saturation, flux, recharge rate on the surface nodes

No	x	z	Total head	Pressure head	Saturation	node flux	recharge
	m	m	m	m	-	m3/s	mm/y
1	0	0.0	0.0	0.0	1.00	-7.52E-06	-791
2	600	6.0	6.0	0.0	1.00	-9.22E-06	-485
3	1200	12.0	12.0	0.0	1.00	-6.18E-06	-325
4	1800	18.0	18.0	0.0	1.00	-4.67E-06	-246
5	2400	24.0	24.0	0.0	1.00	-3.60E-06	-189
6	3000	30.0	30.0	0.0	1.00	-2.59E-06	-148
7	3500	35.0	35.0	0.0	1.00	-1.85E-06	-117
8	4000	40.0	40.0	0.0	1.00	-1.46E-06	-92
9	4500	45.0	45.0	0.0	1.00	-1.10E-06	-69
10	5000	50.0	50.0	0.0	1.00	-7.69E-07	-49
11	5500	55.0	55.0	0.0	1.00	-4.45E-07	-28
12	6000	60.0	60.0	0.0	1.00	-1.03E-07	-7
13	6500	65.0	65.0	0.0	1.00	3.09E-07	20
14	7000	70.0	70.0	0.0	1.00	1.07E-06	68
15	7500	75.0	74.4	-0.6	0.88	1.58E-06	100
16	8000	80.0	77.7	-2.3	0.44	2.06E-06	100
17	8800	101.3	101.0	-0.3	0.93	2.54E-06	100
18	9600	122.7	122.7	0.0	1.00	2.35E-06	93
19	10400	144.0	144.0	0.0	1.00	2.25E-06	89
20	11200	165.3	165.3	0.0	1.00	2.20E-06	87
21	12000	186.7	186.7	0.0	1.00	2.17E-06	85
22	12800	208.0	208.0	0.0	1.00	2.15E-06	85
23	13600	229.3	229.3	0.0	1.00	2.17E-06	85
24	14400	250.7	250.7	0.0	1.00	2.24E-06	89
25	15200	272.0	272.0	0.0	1.00	2.48E-06	98
26	16000	293.3	290.0	-3.3	0.27	2.54E-06	100
27	16800	314.7	304.9	-9.8	0.20	2.54E-06	100
28	17600	336.0	316.8	-19.2	0.20	2.54E-06	100
29	18400	357.3	325.5	-31.8	0.19	2.54E-06	100
30	19200	378.7	331.0	-47.7	0.19	2.54E-06	100
31	20000	400.0	333.3	-66.8	0.19	1.27E-06	100
			Outflow Total			-3.95E-05	-62.34
			Inflow Total			3.95E-05	62.34

3. MEASUREMNT OF UNSATURATED SEEPAGE PARAMETERS FOR ROCKS

For the projects of petroleum gas storage in underground cavern and those of geological disposal of radioactive waste, the measurement of unsaturated parameters for rocks is indispensable but the measurement data are little and the measurement method is not established. The author studied the measurement methods.

3.1 Current status of understanding unsaturated seepage parameters for rocks

The governing equation of ground water flow is shown as Eq.1. It is usually called "Rechards equation". The unsaturated parameters issued here are $C(\theta)$ and $kr(\theta)$ in the equation. They are function of volumetric water content or saturation. $C(\theta)$ is expressed as Eq.2. The relation between ψ and θ is known as moisture characteristic curve(MCC). $C(\theta)$ is differential value of volumetric water content θ by suction ψ. It means measuring $C(\theta)$ is same as measuring MMC.

$$(\alpha Ss + C(\theta))\frac{\partial h}{\partial t} = \frac{\partial}{\partial x_i}\left(ks_{ij}k_r(\theta)\frac{\partial h}{\partial x_j}\right) + Q \quad (i, j = 1,2,3) \qquad (1)$$

$$C(\theta) = \frac{\partial \theta}{\partial \psi} \qquad (2)$$

where, h : total head[m], x_j : Cartesian coordinate [m], t : time[s], α : switching parameter <in the case of saturated(α=1), in the case of unsaturated(α=0)[-]>, Ss : specific storage[m^{-1}], θ : volumetric water content[-], $C(\theta)$: specific water capacity[m^{-1}], ks_{ij} : tensor of saturated permeability[m s^{-1}], $kr(\theta)$: relative permeability[-], Q : source and sink term[s^{-1}] , ψ : suction[m]

In many cases, the MCC and relative permeability(kr) are expressed by van Genuchten's equation (van Genuchten 1990, VG equation) shown below. In the equations blow, VG parameter m and n are independently treated. The subscript 1 means for MCC, the subscript 2 means for kr.

$$Se = \frac{\theta - \theta_r}{\theta_{sat} - \theta_r} \qquad (3)$$

$$Se = \left\{1 + |\alpha\psi|^{n_1}\right\}^{-m_1} \quad (4), \quad \psi = \frac{1}{\alpha}\left(1 - Se^{-1/m_1}\right)^{1/n_1} \quad (4')$$

$$k_r = Se^{\frac{1}{2}}\left\{1 - \left(1 - Se^{1/m_2}\right)^{m_2}\right\}^2 \qquad (5)$$

$$m_i = 1 - \frac{1}{n_i}, \ (0<m_i<1, n_i>1, \ i = 1,2) \qquad (6)$$

where, Se : effective saturation[-], θ_{sat} : saturated volumetric water content[-], θ_r : residual volumetric water content[-], α : parameter of VG equation[m^{-1}], m_i,n_i: parameter of VG equation[-], i=1 is for MCC, i=2 is for kr

The number of measured data of MCC and kr for rocks are less than that for soils. The author searched the measured results published and arranged them using VG parameters in Table1. In the table, rock type, porosity and saturated permeability are shown with VG parameters in the table.

3.2 Measurement of MCC

The suction of the Shirahama sandstone (Takahashi et al. 2004) for MCC are measured by three different method. For lowest suction range, the soil column method was applied. For higher suction range, the pressure plate method was applied. For the highest suction range, the psychrometric method was applied. The measured results are plotted in Fig.4. The plotted results show us the data measured by different methods are continuous and consistent. The plotted data are approximated using VG equation. The parameters of VG equation are namely, n_1=1.24, m_1=0.192, α=0.01[m^{-1}].

In Fig.4, the estimated suctions are plotted using the mercury injection data (Takahashi et al. 2004) based on the capillary effects. The difference between measured suctions and estimated suctions is small at high saturation, it becomes larger as saturation decrease. The difference implies the difference between matric suction and capillary suction.

Table.2 measured MCC and kr for rocks

parameters	porosity	saturated permeability	moisture charactice curve			relative permeability	
		k_{sat}	α	n_1	m_1	n_2	m_2
stone type	%	m/s	m^{-1}	–	–	–	–
mudstone 1	58	1.7E-09	0.300	1.08	0.074	1.15	0.130
mudstone 2	30	1.0E-09	0.300	1.67	0.400	$=n_1$	$=m_1$
mudstone 3	–	–	0.200	1.67	0.400	$=n_1$	$=m_1$
mudstone 4	20	1.6E-12	0.008	2.44	0.590	$=n_1$	$=m_1$
mudstone 5		1.1E-12	0.004	1.75	0.430	$=n_1$	$=m_1$
mudstone 6	36.5	1.0E-09	0.800	3.33	0.700	$=n_1$	$=m_1$
mudstone 7	–	–	0.800	2.00	0.500	$=n_1$	$=m_1$
argillaceous 1	22.5	5.0E-14	0.00035	1.7	0.412	–	–
argillaceous 2	15-20	2.0E-13	0.00018	3.50	0.714	–	–
sandstone 1	15	1.0E-10	0.010	1.24	0.192	3.00	0.667
tuff 1	45-50	9.9E-08	0.018	14.0	0.929	–	–
andesite 1	10.4	1.0E-11	0.060	3.57	0.720	$=n_1$	$=m_1$
granite 1	0.82	1.25E-12	0.010	2.26	0.558	$=n_1$	$=m_1$
granite 2	0.67	–	0.014	2.09	0.522	$=n_1$	$=m_1$
granite 3	1.006	1.0E-13	0.035	1.55	0.355	–	–

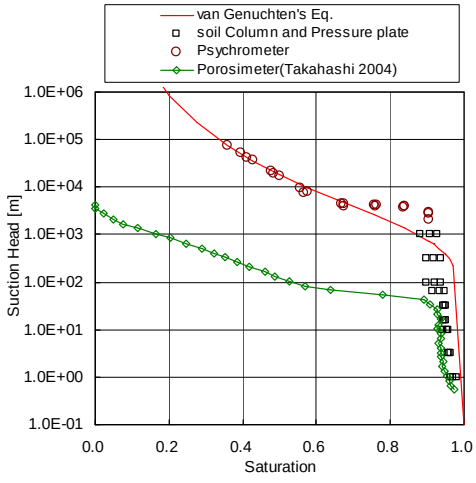

Fig.4 Settlement transition estimated based on the water content change

3.3 Measurement of relative permeability kr

The relative permeability kr were identified by two types of evaporation laboratory experiments using the Shirahama sandstones.

One experiment(as test-1) was transient test in which the evolutions of suction in a test stone induced by the moisture evaporation were measured. The all surfaces of a test stone were sealed with impermeable material to prevent evaporation without one end tip of the column. The end tip without sealing allows the evaporation from the stone. The kr function was identified using an inversional calculation focusing on the measured suction profile. The measured suction and the results of calculation was plotted in Fig.5. The kr function was expressed by Eq.5. The applied parameter n2 was shown in Fig.5. Fig.5 implied the value of n2 should be from 3 to 5.

Another experiment(test-2) was steady state test in which the one dimensional moisture distribution in test specimen was measured. The function of kr was also identified using an inversional calculation focusing on the measured suction profile. The measured water content were plotted as saturation in Fig.6, and calculated saturation distribution were also plotted the same graph. The results implied the value of n2 should be from 3 to 5.

The different two experiments showed same n2 value. The coincidence of the identified kr courve suggest us the reliability of the experiments and the identified results.

3.4 Methods of measuring MCC and kr for Rocks

In this section, the methodology of measuring unsaturated seepage parameter MCC and kr for rocks were presented. The presented method required preparation of saturated specimen of which the saturated permeability and porosity are known. At the first step, MCC measurements are suggested, and secondly, one dimensional evaporation test and the inversional calculation to identify the kr function using preliminary measured MCC. Two kinds of effective experiments are available.

4. ESTIMATION METHOD OF GROUND SETTELMENT USING THE RESULTS OF GROUNDWATER FLOW SIMULATION

Most large cities in Japan are located at river mouth areas, and the areas of the cities are not large and land-use prices are high. So, underground utilization is required. The geology near the river mouth is characterized by high groundwater level and three dimensionally complicated structures composed of sandy layers and clay layers. To develop underground space in such area, preliminary evaluations of excavation effects on the groundwater level and on the settlement of the

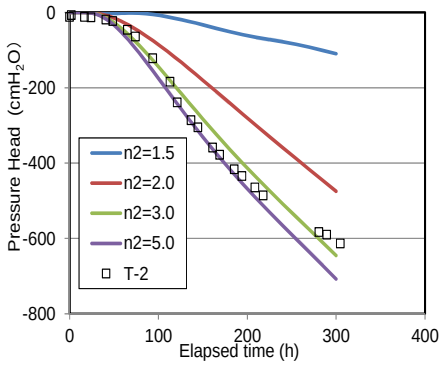

Fig.5 Transition of pressure head(suction) at test-1

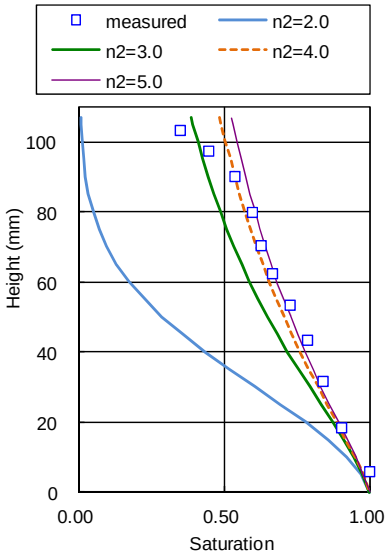

Fig.6 Saturation distribution (test-2)

surrounding field are required. Beside the influence evaluation of construction works including excavation and drainage, efficient counter-measures and appropriate construction planning to prevent inadequate settlement are indispensable. For that requirement, a simple settlement evaluation system using groundwater flow simulation and spreadsheets calculation was built. By applying the system to a three-dimensional model, its validity was examined (Imai, 2004) and confirmed. Furthermore, the system was applied to an actual construction planning. In this presentation, outline of the system is explained, and the process and results applied to the actual construction program are shown hereafter.

4.1 Methodology of settlement calculation

The decreases of pore pressure are calculated as a difference of the simulated pressure under condition before construction, and the simulated pressure under condition during or after construction. For each cell of groundwater flow simulation model on the spreadsheets prepared for settlement calculation, the settlement is calculated based on following equation:

$$S = m_v \cdot H \cdot \Delta p \qquad (7)$$

where, S: settlement of a cell, m_v: coefficient of volume compressibility, H: height of a cell, dp: increase of effective pressure at the center of the cell.

The surface settlement is the value vertically summarizing the settlement of all cells composing a vertical column from the bottom to the top (surface) of the model as expressed in Eq (2). The image of settlement summarization is shown in Fig.1.

The coefficient of volume compressibility m_v is obtained from the results of laboratory consolidation test on clays. For sandy soils, the equivalent m_v is estimated by modulus of deformation E or using the relationship curves between pressure and void ratio suggested by B.K. Hough (JH 1998). The relationship curves are classified into five type curves depending on the N-values. Therefore, in this estimation system, input of mv is required for clay soils only, while E or N-value is required for sandy soils. In actual calculation, the model region is classified into some soil type groups. The grouping is set beforehand in the groundwater flow simulation. Therefore, in evaluating settlement we have to set independent soil type groups instead of the same hydraulic conductivity as in modeling for MODFLOW simulation.

Allow one blank line before and after each illustration provided in the manuscript.

$$S = \sum_i S_i = \sum_i m_{v_j} \cdot H_j \cdot dp_j \qquad (8)$$

4.2 Application to the actual construction site

4.2.1 Outline of the construction site

The developed settlement evaluation system was applied to an actual road tunnel construction site. The construction site is located on the seaside, and the groundwater level is high. The dimension of the excavation area is 20 meters deep, 150 meters long and 40 meters wide. The planar layout of the construction site is shown in Fig.8, and the vertical section of the site and the sediment condition is shown in Fig.9. The excavated area is retained by steel sheet pile wall installed to the bedrock about six meters deeper than the excavation bottom. The wall is expected to keep out groundwater leakage. The wall is drawn and written as “Impervious wall” in Fig.8 and Fig.9. Deep wells are installed inside the excavation area, while recharge wells are installed around the excavation area. Groundwater level monitoring wells and settlement monitoring gauges are set around the construction site. The installed wells and gauges are shown in Fig.8.

The subsoil consists of bedrock (Icg) with some damaged zones, diluvial sand and gravel (Dsg), alluvial clay (Ac), alluvial sand (As1, As2, As3) and banked soil (B).

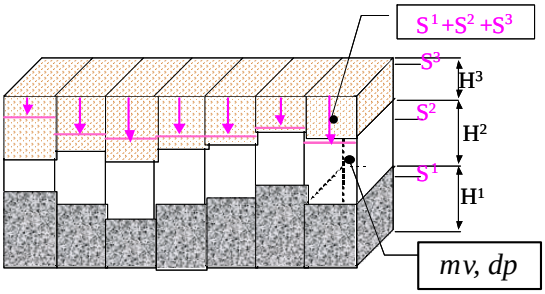

Fig.7 Image of settlement calculation
The number N in equation (2) is 3 in this image.

The Machineries are set near this excavation site. The alluvial clay (Ac) is inferred to cause harmful settlement. To understand the excavation effect, the groundwater level monitoring wells and settlement observation wells are set around the excavation site.

4.2.2 Design of countermeasures against settlement

To select the most effective countermeasures, the evaluation system was applied. The application was carried out in the following manner. Firstly, the hydraulic characterization of the site was conducted based on groundwater flow simulations, utilizing the response of tide in monitoring wells and the results of pumping tests. The characterization clarified the hydraulic parameters of the sandy layer and the bedrock, as well as sealing performance of the retaining walls and the bedrock mass. Second, the excavation and drainage influence on groundwater flow was simulated by MODFLOW. The simulation was carried out at the steady state condition. Third, settlement estimation was completed. Forth, case studies of the above mentioned countermeasures were carried out. At each case, detail design such as well location, depth of curtain grouting and thickness of bottom improvement were performed by the system.

Parameters for settlement calculation are summarized in Table 3. The coefficient of volume compressibility m_v is given by the results of laboratory consolidation test for clay only, while for sandy soils the reciprocal numbers of deformation modulus are applied.

Fig.10 shows the distribution of estimated settlement of ground surface around the excavation for the condition of no countermeasure. The area settlement is extendedly coincided with the zone where the Ac layer is thick.

Fig.11 shows profiles of settlement estimated along the section of a-a’ for five different conditions, namely 1) No countermeasure case; 2) No countermeasure case in the clay layer (Ac); 3) Bottom improvement case; 4) Curtain grouting case; and 5) A case combining bottom improvement and recharge well. The “No countermeasure case in clay layer” implies the settlement occurred just in the clay layer (Ac). The

"No countermeasure case" implies the total settlement induced from all involved sediments. It is shown that the settlement of clay layer shares more than 50 percent of the total settlement.

The results indicated that among the examined cases, the countermeasure combining bottom improvement with recharge well is most effective. Thus it was selected to employ.

4.2.3 Measured data and simulated results

In the actual construction, the deep wells were set to decrease water level in the excavated area, and the countermeasure combining bottom improvement with recharge wells was applied to prevent harmful settlement outside the excavated area. The pumping up rate of the deep wells and injection rate of the recharge wells were measured, and the settlement near the machineries were measured, and the measured data and corresponding simulated results are shown.

Arrangement of settlement measurement at station JW1 can be seen in Fig.8. At the station, four measurement points were set: one at the surface, and each in the middle of layers As1, As23 and Ac as shown in Fig.8. The measured data at each point indicates the amount of settlement induced by the soil thickness involved between that point and the bottom of Ac layer. For example, data from point As23 represents settlement due to compression of entire layer Ac and the lower haft of layer As23. And the point Surface shows the total settlement due to layers B, As1, As23 and Ac all together.

Beside that, the difference in settlement values for two adjoining points indicates the change in thickness of the soil involved between those two points.

By using this evaluation system, settlement is calculated based on the Eq.1, which require the thickness of layer, coefficient of volume compressibility mv and increase in effective transient pressure, which is obtained from groundwater simulation. It should be note that, although this evaluation system was originally developed for applying to steady state condition of ground water, however it was thought that it would be effective to check the applicability of the system to unsteady condition. Therefore, in this application, settlement was calculated based on transient pressure obtained from unsteady groundwater simulation.

The measured and estimated settlement values are shown in Fig.9. About the measured data, settlement amounts at Surface point and As1 point are almost the same, and the difference between As1 and As23 is very small. These measured results suggested that deformations of B (Banked soil), As1 and As23 are very small, and most of the settlement arises in clay layer Ac. It is considered that the groundwater head drawdown occurred in Dsg layer just beneath Ac layer, and thus mainly acted on Ac layer. On the other hand, as Ac layer works like an impermeable layer, it reduced the pressure changes in upper layers as As23, As1 and B.

About the estimated data, differences in settlement values from Surface, As1 and As23 points are small and indicate almost the same tendencies as measured data at each of these three points, respectively. However, the estimated settlement values are more than twice higher than the measured values. It was suggested that the difference in settlement between estimated and measured values was caused by a corresponding difference in the drawdown, because the estimated drawdown in water level at observation well WLR-09 is about twice of the measured drawdown.

4.2.4 Settlement evaluation based on the water budget

The above-mentioned estimation of settlement (i.e. Eq.7) is based on deformation characteristics of soils. On the other hand, settlement can also be estimated based on the water budget for saturated clay soils.(Ishihara 1988) The amount of water drained out due to the pressure change coincides with the pore volume change of the soil. It suggests that, for saturated clay layer, settlement can be estimated based on the volume of drained water. The transient change of drained water from a cell of groundwater simulation model can be calculated, from that settlement is estimated from the calculated volume of drained water.

Estimated settlement profiles of clay layer Ac are shown in Fig.14 with measured values. These different profiles were estimated based on different hydraulic parameter specific storage Ss. The approximated curve of measured data is also plotted. The estimated settlement profiles based on water budget are more appropriate than that estimated based on Eq.1 because they are more closer to measured data than the estimated profiles based on Eq.1 are. The reason why the estimated results based on the water budget is closer to the actual settlement than that based on Eq.1 is considered that since actual flow rates at deep wells and recharge wells were applied to the boundary condition of the groundwater simulation, the flow rates directly affect the water budget, then the settlements derived from water budget are close to the actual values. On the other hand, the settlement derived from Eq.1 depends on the pressure change, which was derived from groundwater simulation and may be affected by many parameters such as hydraulic conductivity setting and so. The simulated groundwater level differed from the actual value was shown in Fig.14 (WLR-09).

It is suggested that, settlement estimation based on water budget is effective in case induced settlement is mainly from saturated clay layer.

For road tunnel construction where the ground is composed of soft sediments with high water level, groundwater management plans should be made to keep the excavation safe and dry, and to avoid harmful settlement around the construction site. A simple settlement evaluation system utilizing the data set of groundwater flow simulation was developed to design countermeasures. The system was applied to an actual construction design, and efficiency of the system was examined.

The accuracy of the evaluation system was examined by comparison of evaluated data with measured data such as on groundwater head and settlement. The evaluated and measured data were not completely coincided, but the differences were considered to be in our acceptable range. The tendency of variation of the evaluated data was similar to that of measured data. It implied that the system could evaluate the nature of groundwater and soils appropriately.

Application of the evaluation system to an actual planning showed that the system was effective to compare alternative construction plans in a given condition, and to make construction plans. The system enabled us to make decisions quickly considering both groundwater and settlement effects, allowing to complete the construction safely.

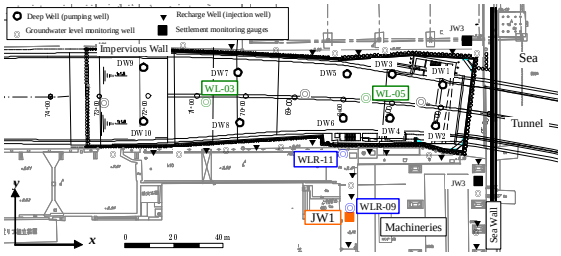

Fig.8 Planar layout of the construction site

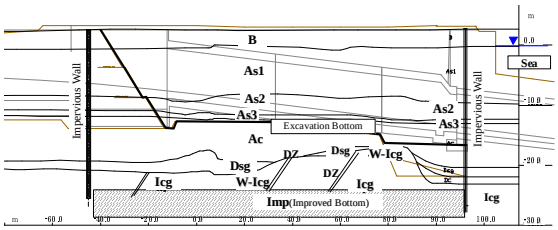

Fig.9 Vertical section and sediment condition

Table3 Material properties applied for geological groups

Group number	Soil type	Symbol	Hydraulic Conductivty (m/s)	Submerged Density (g/cm^3)	N-value	E (kN/m^2)	m_v (m^2/kN)
1	Banked soil	B	1.0E-05	1.0	35	1.0E+04	-
2	Alluvial sand	As1	7.0E-06	0.9	22	1.1E+04	-
3	Alluvial sand	As23	4.0E-06	0.9	10	1.1E+04	-
4	Alluvial Clay	Ac	1.0E-09	0.6	6	6.0E+03	2.0.E-04
5	Sand and Gravel	Dsg	1.0E-05	1.0	28	1.1E+04	-
6	Weathered Base Rock	W-Icg	5.0E-05	1.5	50	9.0E+04	-
7	Base Rock	Icg	5.5E-06	1.5	50	2.5E+06	-
8	Impervious Wall	RW	1.0E-10	2.0	50	2.5E+06	-
9	Fracture Zone	DZ	5.5E-06	1.2	50	9.0E+04	-
10	Diluvial Clay	Dc	1.0E-09	0.7	28	1.1E+04	-
13	Improved Bottom	Imp	5.0E-07	1.0	50	1.1E+04	-

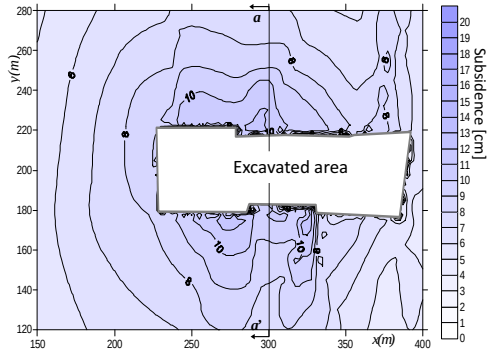

Fig.10 Contour map of settlement (in case of no countermeasure)

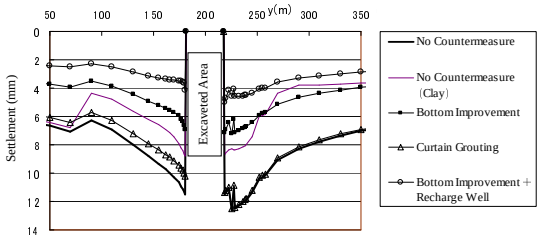

Fig.11 Profiles of simulated settlement considering various countermeasure effects

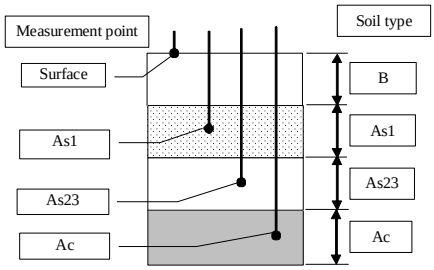

Fig.12 Image of Measurement points

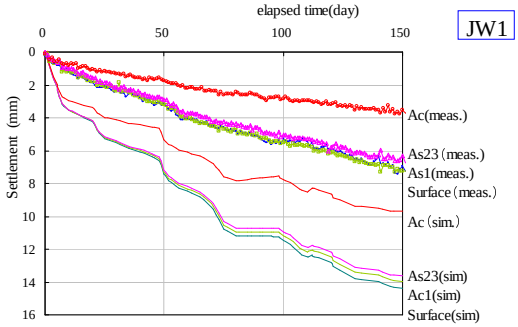

Fig.13 Settlement transition, measured and estimated

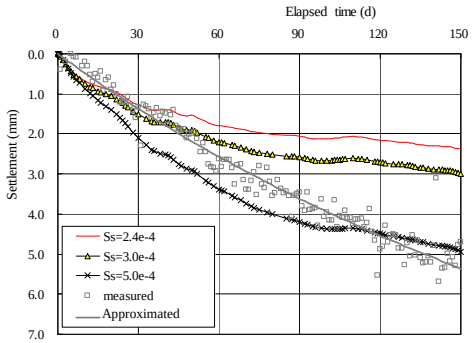

Fig.14 Settlement transition estimated based on the water content change

5. SIMULATION METHOD FOR LONG TERM REGEONAL GROUNDWATER FLOW CHARACTERISTICS CONSIDERING THE CHANGS OF HYDROGEOLOGICAL ENVIRONMENTS

For the appropriate evaluation of long term evolution of regional groundwater flow characteristics, the appropriate modeling procedures for heterogeneous hydrogeological features and changing boundary conditions. To match simulation method with such demands, two steps of studies were carried out. For the first step, the applicability of the developed FEM groundwater simulation was examined by the comparison between the measured and simulated data from the in situ field experiment focusing on the effects of shaft excavation on the nature of groundwater flow. For the second step, newly devised simulation method was proposed and the efficiency of the new method was presented with the simulated result applied to two dimensional model with long term geological topological deformation.

5.1 Groundwater simulation applied to the Shaft excavation experiments

5.1.1 Shaft excavation experiment

In the shaft excavation experiment, a shaft of 6meters in diameter and 150m in depth was newly excavated. The shaft was constructed in the sedimentary sequence and hydrological monitoring was conducted to understand the hydrological effects of the shaft excavation.

The experiment was carried out at the hilly area of elevation from 250m to 320m above sea level. The geology of the area is composed of basement granite and a series of the Quaternary sediments. The sediments are stratigraphically divided into two groups, the Mizunami group pf Miocence age and Seto group of Plio-Pleistocene age. The images of the geology and the underground structures were shown in Fig.15. In the area, a fault, called Tsukiyoshi Fault extends almost center of the area with a strile N80^{o}E and 60^{o}SE. The fault cuts the Mizunamigroup and is concealed by the Seto Group. The displacement is about 30m.

There already existed the Research Shaft and Galleries before the new shaft construction expressed as Experiment shaft in Fig.15.

The shaft excavation schedule is illustrated in Fig.16. In Fig.16, the vertical section of the new shaft is drawn on the left side, the progress of the excavation front is illustrated as a graph showing the relation between time and the depth of the excavation front on the right side of Fig.16. The new shaft was planed to be excavated in 500days.

Around the experimental shaft more than ten monitoring boreholes were set and hydraulic head had been monitored before and during the excavation. The multiple monitoring sections were set, and they enable us to confirm the distribution of hydraulic head distribution along the borehole.

5.1.2 Numerical modeling

To simulate groundwater behavior affected by the shaft excavation, the numerical model for FEM simulation of groundwater flow was constructed. The configuration of the model was shown in Fig.17. The size of the model is about 300mx300mx300m. The model consists of 3133elements and 3924nodes. The model region was divided into 12 hydrogeological groups based on the geological features such as the formations and fault, and the results of preliminary hydraulic investigations. The model was shown in Fig.17.

The boundary conditions were determined based on the preliminary hydrological investigations. The side boundaries are constant head referring the measured head in the monitoring boreholes.

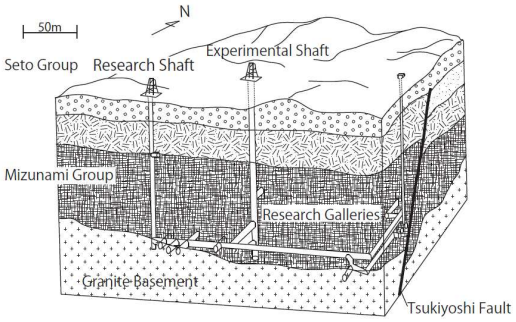

Fig.15 Perspective view of the experimental site with geological structure and underground facilities

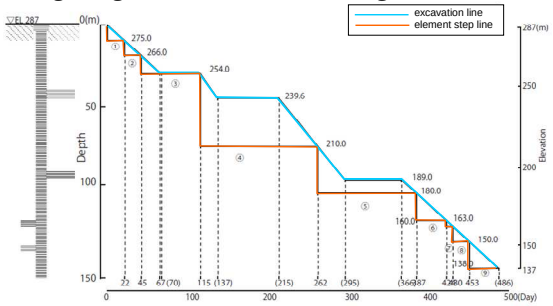

Fig.16 Experimental shaft and excavation schedule

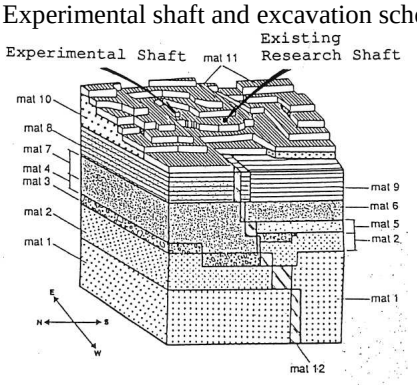

Fig.17 FEM Numerical model classified based on the hydrogeological division from mat1 to mat12

The recharge rate 0.5mm/d was set on the model surface based on the water budget investigations during a year.

The initial condition was set as the total head on each nodes calculated considering the boundary conditions and the existing research shaft and galleries at steady states. The validity of the initial condition was examined referring the measured and calculated inflows into the existing research shaft and galleries.

5.1.3 Simulated results and the measured data

The transient groundwater simulation considering the shaft excavation effects were carried out by the control of the boundary condition setting on the nodes located on the wall and bottom of the excavated shaft. The boundary condition set on the shaft wall and bottom was the Direchlet type boundary condition (i.e. head fixed boundary condition). The control of boundary heads was executed referring the excavation schedule shown in Fig.16 and the saturation of the boundary nodes. The control method was developed for this experiment mentioned chapter 2, and that could prevent the reflex flow from the surface of the shaft to surrounding formations.

Some of the simulated results are presented and compared with the measured data below.

The total head distribution in the vertical section cutting the experimental shaft at the arrival time of the excavation face on the shaft bottom is shown in Fig.18. The equi-head lines are concentrated at the shaft bottom, it means the high groundwater velocity is induced by the excavation.

Fig.19 show the comparison between measured and simulated total head distribution along the monitoring boreholes. The trends of head distribution decreasing in the downward and lowest head at EL150m coincide with measure and simulated results.

Fig.20 shows the relation between decrease in head and distance from the experimental shaft on the plane of EL210m.The elevation 210m is at almost equivalent to the center depth of the experimental shaft. The plots indicate that the decrease in the head becomes smaller with increasing the distance from the shaft and that the simulated results show the good agreement with the measured data. The measured and simulated results suggest us the affected area on head decrease might be within a hundred meters or so.

The comparison of measured and simulated transition of head of a point at EL210m is shown in Fig.21 with the transition of the excavation front (shaft bottom). The measured and simulated head transition show good agreement. This agreements suggests us the efficiency of the boundary condition setting on the nodes located on the wall and bottom of the excavation shaft.

The simulated and measured evolution of inflows into the experimental shaft and the existing shaft and galleries are plotted in Fig.22. The lower graph of Fig.22 is the transition of excavation front.

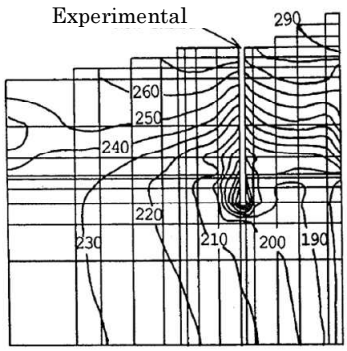

Fig.18 Settlement transition estimated based on the water content change

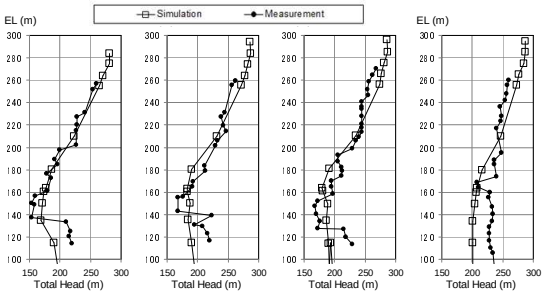

Fig.19 Distribution of Total head along the monitoring Boreholes at the final stage of excavation (530days after the excavation start)

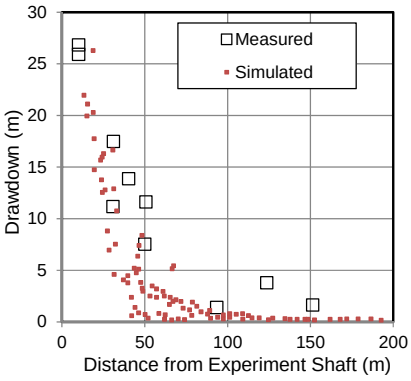

Fig.20 Relation between decrease in head and the distance from the experimental shaft

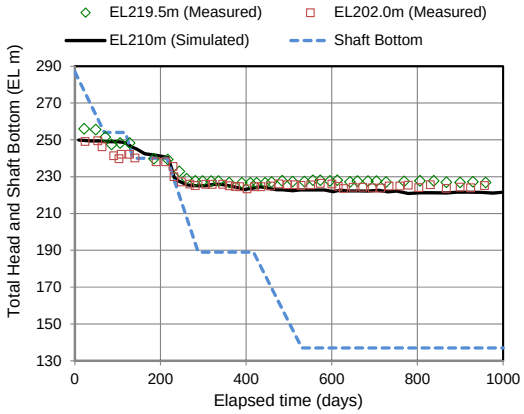

Fig.21 Transition of head at a point at EL210m

The simulated inflow rate is 1.5-2.0 times as much as the measured one. Both the simulated and measured inflow rate into the experimental shaft increased as the excavation proceeded.

The inflow into the experimental shaft tends to increase with the excavation. The value of the measured inflow into the existing research and shaft and galleries fluctuating, but it is almost constant on average during the excavation. The simulated value is also almost constant.

5.1.4 Applicability of the modeling methodology and the numerical modeling

A methodology of hydrological evaluation was applied to the shaft experiment. In this application, the evaluation of the impact on the groundwater flow natures by the shaft excavation was mainly focused. The applicability was confirmed by the comparison between measured and simulated results. The comparison shows good agreements on the change of head, inflow rate into the new shaft and the existing shaft and galleries.

The agreement of the simulated results with the measured data suggested us the efficiency and applicability of the simulation method and the hydrological evaluation methodology applied to this experiment.

5.2 Simulation method of groundwater flow considering the long term evolution of geological environment

In order to understand the characteristics of regional groundwater flow and the nature of deep groundwater, it is indispensable to take account of the effects of long term evolution of geology on the characteristics of groundwater flow. The evolution means the deformation of geological structures and the shape of the ground surface. The author devised the new modeling system which can satisfy the necessities.

5.2.1 Sequential Modeling System of geological evolution impact on groundwater flow

The newly devised system is named “Sequential Modeling System of geological evolution impact on groundwater flow (SMS)”.

At the beginning, the duration for the simulation should be determined, and the duration should be divided into some time steps. Following to the time steps setting, a series of geological models related to the geological ages(time steps) shown as Fig.23 are required. The series of geological models is called “geomodel”. The numerical models for groundwater flow are made referring the geomodel at the corresponding geological ages. The numerical model can be made independently, no relation between the ages are required in this system. The groundwater simulation can be independently executed with the boundary conditions reflected the sea level and recharge rate corresponding to the modeling ages. Though the independent modeling, the initial condition should be set in accordance with the hydrological transition. The initial condition setting is the key issue in this sequential calculation system.

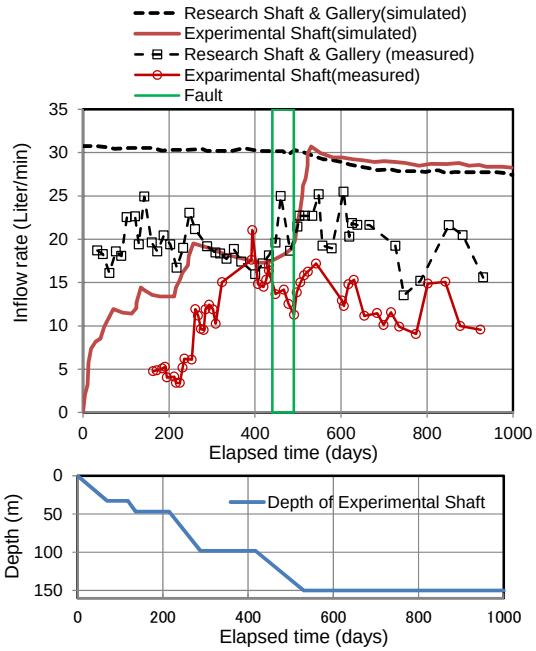

Fig.22 Settlement transition estimated based on the water content change

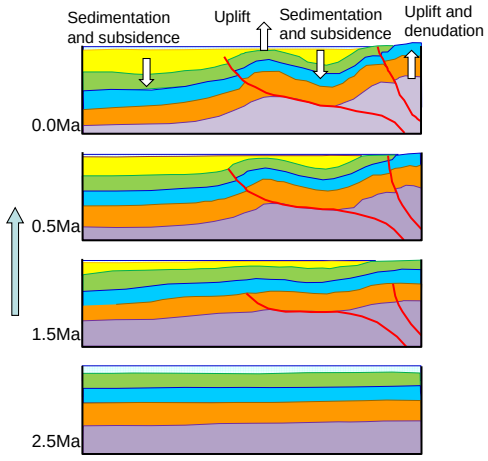

Fig.23 Evolution of geology and topography (geomodel)

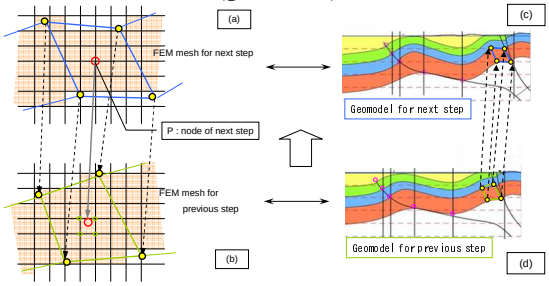

Fig.24 Settlement transition estimated based on the water content change

The method of initial condition setting is illustrated in Fig.24. The lattice drawn in Fig.24(a)(b)means the mesh lines of FEM model for groundwater flow simulation. The crossing points are nodes of the numerical model, and they require the initial head for transient simulation. The nodes at current time step are related to the points of numerical model at previous time step by the geomodel. The geomodel is composed to organize the evolutions of location in the focusing region of groundwater flow modeling.

5.2.2 Applied result

For an example of the SMS application, the wash out simulation focusing on the salinity concentration is shown.

The shape of the model is just like the model in Fig.23. The model surface is rising from the left side to the right side. The left side is sea, and the right side is hilly area. In this simulation time, the left side area is the area where sedimentation and subsidence are proceeding. The right hilly area is an area where the uplift and denudation are proceeding.

At the initial state, the hole model region was saturated with salinity water having same concentration as to sea water(C=1.0, normalized concentration).In the wash out simulation, the infiltration of fresh water supplied as recharge pushes out the initial salinity water and dilutes the salinity concentration.

The results of the application of SMS are shown in Fig.25. Case1 is a just result of wash out simulation without changing of geology. Case2 is the result which SMS was applied with changing of geology. The distributions of concentration are presented in the vertical section on the right side of the figure. The vertical distributions of concentration in line c-c are presented on the left side.

It is realized that the low concentration zone of Case1 is spreading deeper than that of Case2. The difference is induced by the effect of uplifting. In Case2, high concentration formation is arising from the lower part, the arising prevent the fresh water intrusion into the deeper part.

The simulated result and the phenomena of geological evolution are consistent. The consistency suggests the validity of SMS.

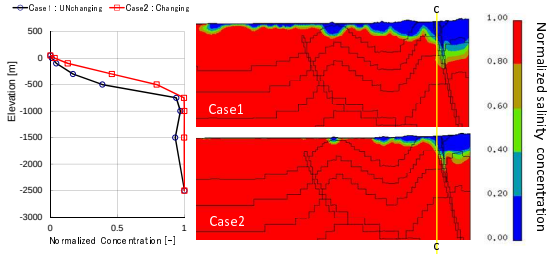

Fig.25 Comparison of salinity concentration with considering the evolution effect and without

6. CONCLUSION

The many kinds of modern problems related to groundwater flow induced by the extension of human activities were treated as the uncertain problem of groundwater flow in varying flow fields. To solve these problems, the following four items were studied. They are study on the methodology of boundary condition in varying flow fields, study on evaluation method for unsaturated seepage parameters in rocks, study on evaluation method of land subsidence utilizing the results of groundwater flow simulation and study on the simulation method to adapt to the changes of long term hydrogeological environments. From the four studies, some kinds of ideas and simulation methods are presented and the availability of the presented ideas and simulation methods were confirmed via application of actual problems and some exercises. Furthermore, the results of the studies showed the applications and utilizing methods of groundwater flow simulation to match the many kinds of groundwater flow problems.

7. ACKNOWLEDGEMENT

This thesis completes the author's results of research and development activities concerning the code development of groundwater flow simulation, the confirmation of the applicability of the developed code via practical application and the measurement of unsaturated seepage parameters for rocks, from the results the author have been engaged the groundwater flow problems in the fields and in laboratory since he was a student of Saitama university.

The author would like to express his sincere appreciations for the kind guidance and encouragements form Professor Kunio Watanabe (Geosphere Research Institute of Saitama university) more than 30 years. The author also would like to thank Associate Professor Tadashi Yamabe(Saitama university), Professor Ken Kawamoto(Saitama university) and Associate Professor Masahiko Osada(Geosphere Research Institute of Saitama university) for many suggestions and warm encouragements.

8. REFERENCES

Imai, H., Eguchi, M., Wakayama, Y. and Yonezawa, A., (2004) "Simple Settlement Evaluation System Based on The Three-imensional Groundwater flow Simulation and Applied Results", *International Conference on Finete Element Models, MODFLOW, and More:Solving Groundwater Problems, Karlovy Vary, Czech Republic*, pp.369-372.

Imai H., Iwataki K., Yoshioto Y., Higuchi A., Eguchi M. (2005): Development of excavation effect evaluation system based on groundwater flow simulation, Annual Journal of Civil

Engineering in the Ocean, JSCE, Vol.21, pp.987-992 (in Japanese)

Imai, H., Shiozaki, I., Yamashita, R., Kurikami, H., Niizato,T. , Maekawa,K. and Yasue, K., (2007) " Trial of the Groundwater analysis Considering the Changing of Hydrogeologecal Environments", *Proceeding of Autumn Lecture meeting of JAGH,* , pp.54-59. (in Japanese)

Imai, H., Amemiya, K., Matsui, H., Sato, T., Saegusa,H. and Watanabe, K., (2013) "The Proposals Relevant to Seepage Flow Simulation in Rockmass around Tunnel under Usaturated Condition -Method for Estimating Unsaturated Seepage Parameters of Stones and Setting of Boundary Condition on Tunnel Wall", *Jounal of JSCE, division C,* Vol. 69, No.3, pp.285-296. (in Japanese)

Ishihara K. (1988): Soil mechanics, MARUZEN, 121-156 (in Japanese)

Japan Highway Public Corporation (JH) (1998): Design manual for soil works, Vol.1, pp. 5-56 (in Japanese)

Takahashi, M., Lin, W., (2004) "Information obtained by mercury intrusion porosimetry and its accuracy", *Journal of the Mining and Materials Processing Institute of Japan*, Vol.120, pp.455-460. (in Japanese)

USGS (2004) USGS Groundwater Software, http://water.usgs.gov/nrp/gwsoftware/modflow2000/modflow2000.html

van Genuchten, M. Th., (1980) "A closed form of A Closed-form Equation for Predicting the Hydraulic Conductivity of Un-saturated Soils", *Soil Sci. Soc, Am. J*., Vol. 44, pp. 892-898,.

Yanagizawa, K., Imai H., Furuya K., Nishigaki M. (1995) "The effects of a shaft excavation on the hydrology of the Tono research filed,Japan", *Journal of Hydrology*, 171,pp.165-190.